RSC Advances

PAPER

View Article Online
View Journal | View Issue

Cite this: *RSC Adv.*, 2017, **7**, 31628

Synthesis of new polyether titanate coupling agents with different polyethyleneglycol segment lengths and their compatibilization in calcium sulfate whisker/poly(vinyl chloride) composites

Yunhua Lu,[a] Weipeng Zhang,[a] Xingwei Li[a] and Shiai Xu *[ab]

Received 30th March 2017
Accepted 14th June 2017

DOI: 10.1039/c7ra03692b

rsc.li/rsc-advances

Six new polyether titanate coupling agents with different polyethyleneglycol (PEG) segment lengths were prepared in this study and were then used to modify calcium sulfate whiskers (CSWs) in order to improve the compatibility between CSWs and poly(vinyl chloride) (PVC). The chemical structure of these coupling agents was characterized by FTIR, Raman, ^{1}H NMR and ^{31}P NMR, and the surface properties of CSWs modified by the coupling agents (mCSWs) were characterized by FTIR, SEM-EDS and XPS. Then, CSW/PVC and mCSW/PVC composites were prepared using a two-roll mill, and their mechanical and thermal properties were characterized to investigate the effects of the PEG segment length of the coupling agents on the performance and compatibility of the composites. The results show that the new coupling agents can significantly improve the compatibility and the interfacial adhesion between CSWs and the PVC matrix, which results in a significant improvement of the comprehensive performance of mCSW/PVC composites. PEG4000 shows the best modification effect on CSWs. Finally, the underlying mechanisms are discussed.

1. Introduction

Polyvinyl chloride (PVC) is one of the most extensively used general-purpose plastics in the construction industry due to its excellent properties such as high mechanical strength, high corrosion resistance and relatively low cost.[1–3] However, it is not exempt from drawbacks such as low modulus, poor thermal stability and impact resistance, which may impose some limitations on its applications.[4,5] Thus, attempts have been made to impart required properties (*e.g.*, toughness, modulus and heat resistance) to the PVC materials by incorporating various fillers into the PVC matrix.[6–8] Various fillers, such as organic elastomers[9–12] and reinforcing agents,[6] as well as inorganic natural fibers,[13,14] whiskers[15–17] and nanoparticles[18–22] have been shown to be capable of improving the comprehensive performance of PVC composites. Calcium sulfate whiskers (CSWs) as a reinforcing filler can dramatically improve the impact resistance, modulus and thermal resistance of PVC composites,[17,23] as they have integrated shape, high intensity, high-temperature resistance and high tenacity. In addition, CSWs are superior to many other whiskers due to their nontoxicity, chemical corrosion resistance, constant size, easy surface treatment and a high performance/price ratio.[24,25]

However, the compatibility between the inorganic fillers and the organic matrix is generally poor, which may impede the transmission of the stress applied to the composite from the matrix to the fillers, and thus may cause premature rupture of the composite.[26] In order to overcome this problem, the inorganic fillers are subjected to surface modification to improve their adhesion to the organic matrix.[27–30] Surface modification can increase the interfacial adhesion strength by increasing the surface tension and roughness or changing the surface chemistry of fillers.[31–33] Recently, Yuan and Cui *et al.* found that CSWs coated by crosslinked polyvinyl alcohol (PVA) or chitosan (CS) greatly improved the tensile and impact properties of CSW/PVC composites, which could be attributed to the good affinity between PVC and PVA or CS molecules coated on the surface of CSWs.[17,23,34–36] Coupling agents are usually used to modify the inorganic fillers to improve their interfacial strength with polymers,[37,38] and the most commonly used coupling agents for this purpose include silane coupling agents,[39,40] titanate coupling agents[41,42] and fatty acids.[43] Monte and Sugerman[44] reviewed the applications of titanate coupling agents in plastic composites and coating, as well as the chemical structures of commercial titanates, the coupling mechanism, and their uses. Hajian *et al.*[42] investigated the effects of titanate as a coupling agent and some particulate nanoscale particles such as TiO_2, $CaCO_3$, and ZnO on thermal and mechanical properties of

[a]*Key Laboratory for Ultrafine Materials of Ministry of Education, School of Materials Science and Engineering, East China University of Science and Technology, Shanghai 200237, China. E-mail: saxu@ecust.edu.cn; Tel: +86-021-64253353*
[b]*School of Chemical Engineering, Qinghai University, Xining 810016, China*

emulsion polyvinylchloride, and the titanate used was an industry grade product with a very complex chemical structure and a short organic chain. Feng-e *et al.*[45] synthesized polypropyleneglycol (PPG) titanates, which were then used to modify $CaCO_3$ particles to fill high density polyethylene, polypropylene and polyvinyl chloride. However, they did not investigate the effect of chain length of PPG segment on the miscibility and mechanical properties of PVC composites.

The use of titanate coupling agents is preferred not only because of their bridge effect between the inorganic fillers and the polymer matrix,[46–49] but also because of their suitability for a variety of inorganic fillers, including fillers having surface hydroxyl groups and fillers such as carbonates and carbon black which can not be modified by silane coupling agents.[50] However, it is sometimes difficult to choose an appropriate titanate coupling agent for a specific composite because of the limited availability of specific commercial coupling agents. It is well known that PVC has a good compatibility with polyether polymers, thus we have previously synthesized a titanate coupling agent with PEG200 segment to modify CSW.[34] However, there are many kinds of polyethyleneglycol (PEG) homologues with different segment lengths or molecular weights. Obviously, the segment length of organic molecules plays a crucial role in the compatibility between the fillers and the polymer matrix, and such knowledge is important to choose an appropriate titanate coupling agent.

The purpose of the present study is to synthesize a series of new polyether titanate coupling agents with different PEG segment lengths and to investigate their effects on the interfacial compatibility and properties of CSW/PVC composites. The polyether titanate coupling agents synthesized using PEG300, PEG600, PEG1000, PEG2000, PEG4000 and PEG6000 are denoted as eTi_{300}, eTi_{600}, eTi_{1000}, eTi_{2000}, eTi_{4000} and eTi_{6000} respectively. Then, CSWs treated by eTi_{300}, eTi_{600}, eTi_{1000}, eTi_{2000}, eTi_{4000} and eTi_{6000} were used to reinforce PVC. The effects of the PEG segment length in the titanate on the compatibility and interfacial adhesion were evaluated based on the morphologies and properties of the CSW/PVC composites. Importantly, our study is among the first to investigate the effects of the segment length of the coupling agent on the interfacial adhesion and properties of the composites.

2. Experimental

2.1. Materials

P_2O_5 (analytically pure), isooctyl alcohol (chemically pure) and dichloroethane (analytically pure) were purchased from Shanghai Lingfeng Reagent Co., Ltd. (Shanghai, China). Titanium isopropoxide was purchased from Aladdin Reagent Co., Ltd. (Shanghai, China). PEG (chemically pure) was purchased from Sinopharm Chemical Reagent Co., Ltd. (Shanghai, China). PVC (SG-5) (particle size: 200–250 μm; intrinsic viscosity: 112 mL g^{-1}; the number of impurity ions ≤ 10; the content of volatile matter ≤ 0.16%; apparent density ≥ 0.54 g mL^{-1}; whiteness% ≥ 84.1) was purchased from Dongguan Dansheng Plastic Materials Co., Ltd. (Dongguan, China). CSWs (average diameter: 1–8 μm; average length: 30–200 μm; melting point: 1450 °C; whiteness% ≥ 98; density: 2.69 g cm^{-3}; pH: 6–8; water-solubility ≤ 1200 ppm (22 °C)) were purchased from Shanghai Fengzhu Trading Co., Ltd. (Shanghai, China). Organic tin, dioctyl phthalate (DOP), glyceryl monosterate (GMS), acrylic processing aid (ACR) and paraffin wax were commercially available and all of them were technical grade.

2.2. Synthesis of polyether titanates

The synthesis of polar polyether titanate coupling agents is shown in Scheme 1. Dichloromethane solvent, isooctyl alcohol and PEG (n(isooctyl alcohol) : n(PEG) = 2 : 1) were added sequentially into a three-necked round-bottom flask fitted with a mechanical overhead stirrer. A certain amount of P_2O_5 was added slowly in batches, and then the mixture was stirred at 60 °C for 2 h. After that, the excess solvent was removed by vacuum distillation, and the obtained transparent liquid was pyrophosphate. Then, a certain amount of titanium isopropoxide and dichloromethane solvent were added sequentially into a three-necked round-bottom flask, and then pyrophosphate (n(titanium isopropoxide) : n(pyrophosphate) = 3.4 : 1) was added dropwise. The mixture was stirred at 90 °C for 2.5 h. After that, the excess solvent was removed by vacuum distillation, and the light yellow and viscid liquid was obtained. The structural formula is as follows:

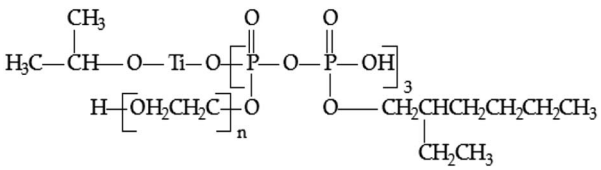
(1)

2.3. Preparation of composites

CSWs modified by eTi_{300}, eTi_{600}, eTi_{1000}, eTi_{2000}, eTi_{4000} and eTi_{6000} were denoted as eTi_{300}-CSW, eTi_{600}-CSW, eTi_{1000}-CSW, eTi_{2000}-CSW, eTi_{4000}-CSW, and eTi_{6000}-CSW, respectively. The modification process was as follows: 3 wt% coupling agents relative to CSWs were pre-hydrolysed in 95 wt% ethanol

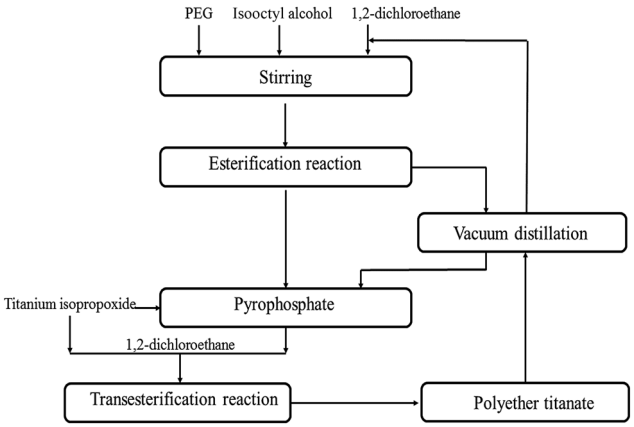

Scheme 1 Synthesis of polyether titanate coupling agents.

solution, and then a certain amount of dried CSWs were added sequentially into a three-necked round-bottom flask fitted with a mechanical overhead stirrer. The mixture was stirred at 75 °C for 4 h, and the obtained products were dried under vacuum at 100 °C for 2 h to remove excess water.

The PVC composites were prepared as described in our previous study:[34] PVC resin (100 phr) was mixed with various contents of CSW or mCSW using organic tin (2 phr) as a heat stabilizer and DOP (4 phr) as a plasticizer. GMS (0.6 phr), ACR (4 phr), and paraffin wax (0.4 phr) were then added. The mixture was mixed thoroughly and then processed using a two-roll mill at 170 °C for 10 min (nip gap: 1 mm; rotating speed: 20 rpm), and the resultant compound was molded into rectangular sheets by compression molding at 170 °C and 10 MPa for 5 min using a plate vulcanizing press. As a control, PVC containing all constitutes except whiskers was processed following the same procedure.

2.4. Characterization and measurements

The Fourier transform infrared (FTIR) spectra were recorded on a Nicolet 6700 FTIR spectrometer (Thermo Fisher, New York, USA) with a scan number of 32 and a resolution of 4 cm^{-1}. The Raman spectra were recorded on an Iuvia Reflex spectrometer (Renishaw, London, UK) at 785 nm at room temperature. The ^{1}H NMR and ^{31}P NMR spectra were recorded on an AVANCE 500 NMR spectrometer (Bruker, Berlin, Germany) at 500 MHz. The surfaces of the samples were characterized by the X-ray photoelectron spectroscope (XPS) on ESCALAB 250Xi (Thermo Fisher, New York, USA) with a Mg Kα photon energy of 1253.6 eV.

The tensile properties were determined using a MTS E44 universal testing machine in accordance with ISO 527, and the notched impact strength was determined using a CEAST 9050 tester according to ISO 179. At least five independent measurements were made for each sample analyzed, and the means were used for further analysis. The dynamic mechanical properties were determined using a TA Instruments Q800 (TA instruments, New Castle, USA) in a three-point bending mode at a vibration frequency of 1 Hz from 25 to 140 °C at a heating rate of 3 °C min^{-1}. The fracture surfaces of the tensile samples were observed under a scanning electron microscopy (SEM, S-4800, Hitachi, Tokyo, Japan). Prior to SEM observation, the fracture surfaces were coated with a thin gold layer.

Vicat softening temperatures (VST) were measured using a VST tester (ZWK1302-B, MTS, Shenzhen, China) in accordance with ISO 306 at a load of 10 N and a heating rate of 120 °C h^{-1}. Thermogravimetric analysis (TGA) was carried out using a Netzsch STA 409PC thermogravimetric analyzer at a heating rate of 10 °C min^{-1} to 600 °C under a nitrogen atmosphere.

3. Results and discussion

3.1. Chemical structure of polyether titanates

Six homologs of polyether titanate coupling agents with different PEG lengths were synthesized in this study. Here, the chemical structure of these six coupling agents was analyzed using eTi_{4000} as an example. Fig. 1 shows the FTIR spectra of the

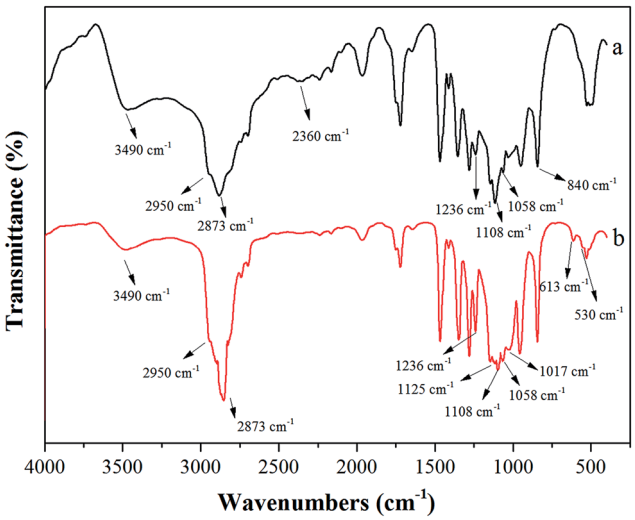

Fig. 1 FTIR spectra of (a) pyrophosphate and (b) eTi_{4000}.

intermediate product (pyrophosphate) and the target product (eTi_{4000}). The broad bands at about 3600–3400 cm^{-1} are assigned to the O–H stretching vibration. The bands in the range of 2980–2800 cm^{-1} are assigned to the C–H stretching of methyl and methylene. The bands at 1125, 1236 and 840 cm^{-1} correspond to the C–O–C, P=O and P–O–P stretching vibration, respectively. The bands at 1058 and 1108 cm^{-1} are assigned to the P–O–C stretching vibration. The band at 2360 cm^{-1} is attributed to the stretching of P–OH, and the new absorption peaks at 1017, 613 and 530 cm^{-1} are attributed to the vibration of P–O–Ti and Ti–O, respectively. The FTIR results prove that a new coupling agent with both PEG segment and isooctyl alcohol group has been successfully synthesized in this study.

Fig. 2 shows the Raman spectra of the intermediate product (pyrophosphate) and the target product (eTi_{4000}). The peaks at 840–860, 930 and 1063 cm^{-1} are assigned to the P–O–P symmetric stretching vibration, P–O symmetric stretching vibration and P–O–C vibration, respectively.[51] The peaks at

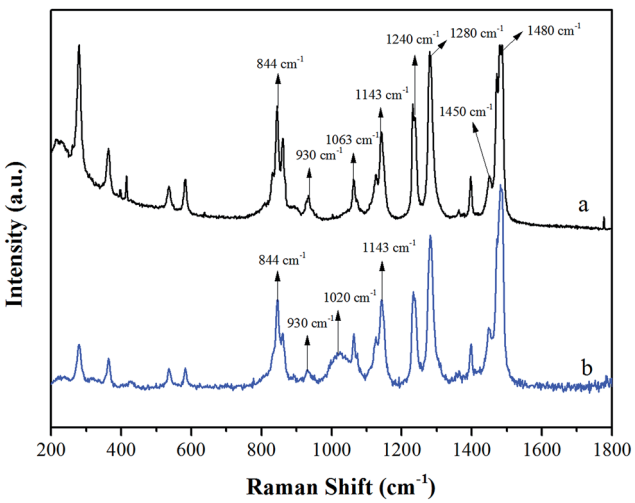

Fig. 2 Raman spectra of (a) pyrophosphate and (b) eTi_{4000}.

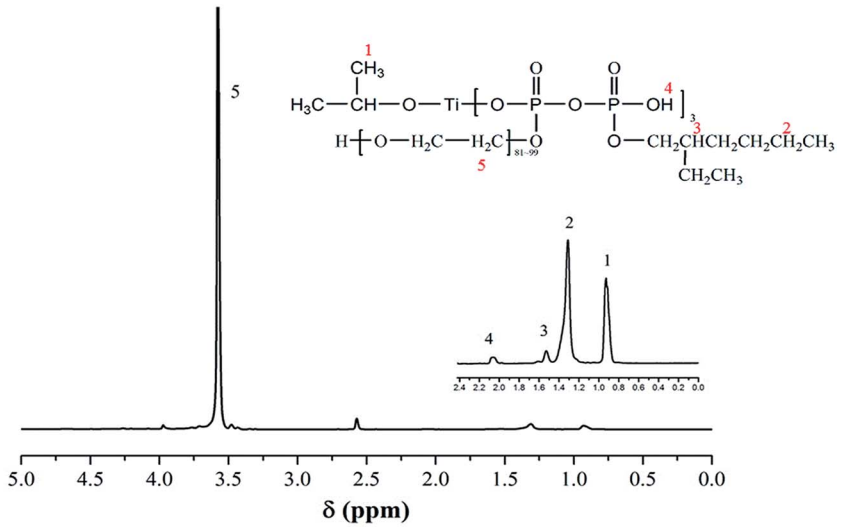

Fig. 3 ^{1}H NMR spectra of eTi$_{4000}$.

1130–1143 and 1240–1248 cm^{-1} are assigned to the C–C stretching vibration and the C–O–C symmetric stretching vibration, respectively.[52] The peak at 1450–1480 cm^{-1} is assigned to the bending vibration of methyl and methylene. The absorption peaks at 200–450 cm^{-1} are assigned to the O–Ti–O bending vibration and the Ti–O stretching vibration.[53] The Raman spectra further confirm the successful synthesis of the new coupling agent with the expected chemical structure.

Fig. 3 shows the ^{1}H NMR spectrum of eTi$_{4000}$, some regions are enlarged to show the significant intensity of the signals, and assignments are given in Table 1. Fig. 4 shows the ^{31}P NMR spectrum of eTi$_{4000}$. The two peaks correspond to the two P atoms shown in the formula. Based on the NMR, FTIR and Raman results, it is evident that the chemical structure of eTi$_{4000}$ is in line with structural formula.

3.2. Characterization of CSWs modified by coupling agents

Fig. 5 shows the FTIR spectra of unmodified CSW and CSW modified by eTi$_{4000}$ (eTi$_{4000}$-CSW). Compared with unmodified CSW, three new absorption peaks are observed at 2950, 2360 and 840 cm^{-1} in the FTIR spectra of eTi$_{4000}$-CSW, respectively, which are the characteristic absorption bands of eTi$_{4000}$. Thus, CSW has been functionalized by eTi$_{4000}$.

Fig. 6a and b show the EDS spectra of CSW and eTi$_{4000}$-CSW, and Fig. 6c and d show their corresponding SEM images, respectively. It can be seen that the morphologies of CSW and eTi$_{4000}$-CSW are similar, indicating that the morphology is not affected by the modification, this may be because the molecular layer of the coupling agents is very thin. The EDS results of CSW and eTi$_{4000}$-CSW are summarized in Table 2. Unmodified CSW is composed of O (44.70 wt%), Ca (30.60 wt%) and S (24.70 wt%), which is approximately consistent with the formula of $CaSO_4$ (Fig. 6c and Table 2). However, eTi$_{4000}$-CSW is composed of O (54.32 wt%), Ca (25.43 wt%), S (20.02 wt%), P (0.19 wt%) and Ti (0.04 wt%) (Fig. 6d and Table 2). Clearly, the presence of the coupling agent on the CSW surface results in an increase in the O content and a decrease in the Ca and S contents. A significant amount of P and Ti elements are also observed on the eTi$_{4000}$-CSW surfaces.

Table 1 Chemical shift assignments and multiplicities of the ^{1}H NMR spectra of eTi$_{4000}$[a]

Signal	Chemical shift (ppm)	Multiplicity	Type of protons
1	0.96	t	$-CH_3$
2	1.29–1.33	m	$-(CH_2)_n-$
3	1.56	m	-CH$_2$-CH-CH$_2$-
4	2.0	s	–OH
5	3.72	m	$-(CH_2CH_2O)_n-$
	3.56	m	-CH-O-
	3.49	m	-O-CH$_2$-

[a] Abbreviations: t: triplet; m: multiplet; s: singlet.

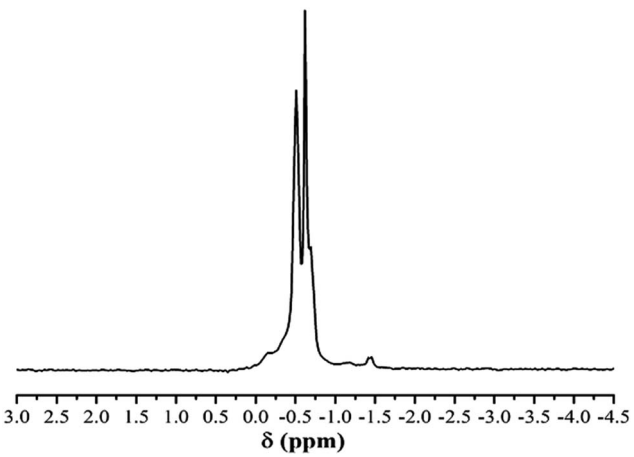

Fig. 4 ^{31}P NMR spectra of eTi$_{4000}$.

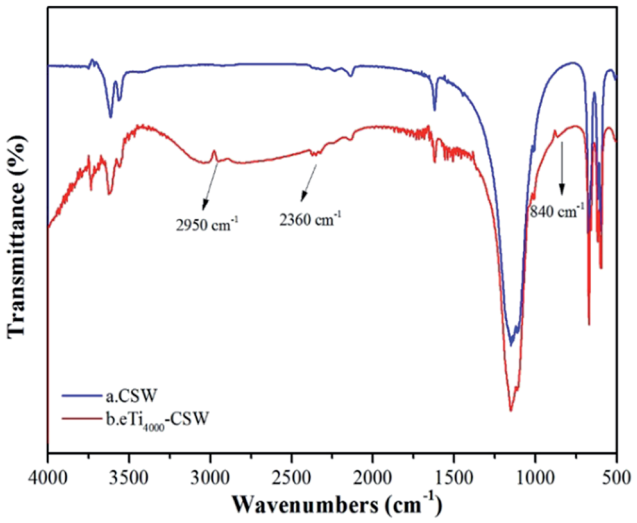

Fig. 5 FTIR spectra of (a) CSW and (b) eTi_{4000}-CSW.

XPS was used to determine the elements and functional groups on the CSW surface. The peaks at about 284.6, 532.0 and 133.2 eV are the C 1s, O 1s and P 2p peaks, respectively.[54–56] The C 1s spectra of CSW and eTi_{4000}-CSW are fitted in order to determine the functional groups on their surfaces. As shown in Fig. 7a and b, the C 1s spectra of CSW can be fitted to two peaks with a binding energy of 284.6 and 286.3 eV, which can be attributed to the C–C and C–O transitions, respectively. Fig. 7 also shows that the C 1s spectrum of C–O transition increases significantly from 15.1% before modification to 47.1% after modification, which can be attributed to the organic segments of the coupling agent. The O 1s spectra of eTi_{4000}-CSW can be fitted to three peaks with a binding energy of 531.7, 532.6 and 532.0 eV, which can be attributed to O–H, O–C and $CaSO_4$ transition, respectively. The O–H bond mainly originates from modified CSW which has crystal water in the modification process and the coupling agent with hydroxyl groups. In addition, P 2p is observed on the surface of modified CSW, which is assigned to the $P_2O_7^{4-}$ transition. Obviously, the XPS results agree well with that of FTIR and SEM-EDS.

Table 2 EDS results of CSW and eTi_{4000}-CSW

	CSW		eTi_{4000}-CSW	
Sample	Weight (wt%)	Atom (at%)	Weight (wt%)	Atom (at%)
O	44.70 ± 12.30	59.50 ± 11.50	54.32 ± 8.00	66.51 ± 8.80
Ca	30.60 ± 5.20	20.20 ± 2.20	25.43 ± 2.50	15.73 ± 2.30
S	24.70 ± 1.60	20.30 ± 2.50	20.02 ± 1.40	17.67 ± 1.20
P	0	0	0.19 ± 0.01	0.07 ± 0.03
Ti	0	0	0.04 ± 0.01	0.02 ± 0.00

3.3. Mechanical performance of the composites

The tensile properties of pure PVC, CSW/PVC and mCSW/PVC composites are shown in Fig. 8. It is clear that mCSW/PVC composites have better mechanical properties than CSW/PVC composite. The polyether (PEG) segment in titanates has a good miscibility with the PVC matrix, and thus the bonding of the PEG segment to the CSW surface could contribute to improving the interfacial affinity of mCSW with the matrix due to the mechanical interlocking between the PEG segments and the PVC molecular chains.[57] Therefore, the tensile performance of mCSW/PVC composites is better than that of unmodified CSW/PVC composite.

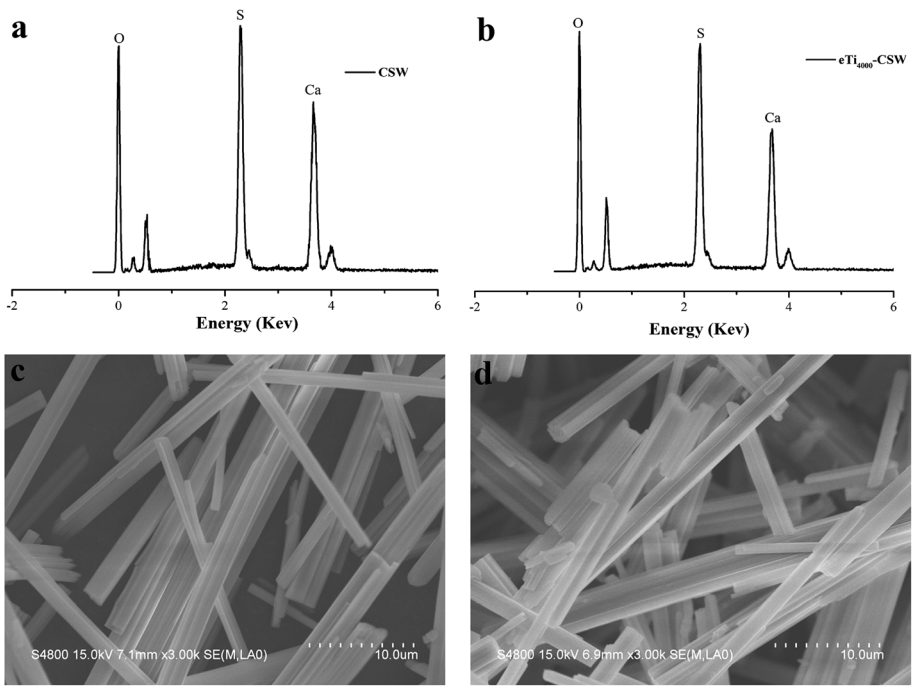

Fig. 6 EDS spectra and surface morphologies of (a and c) CSW and (b and d) eTi_{4000}-CSW.

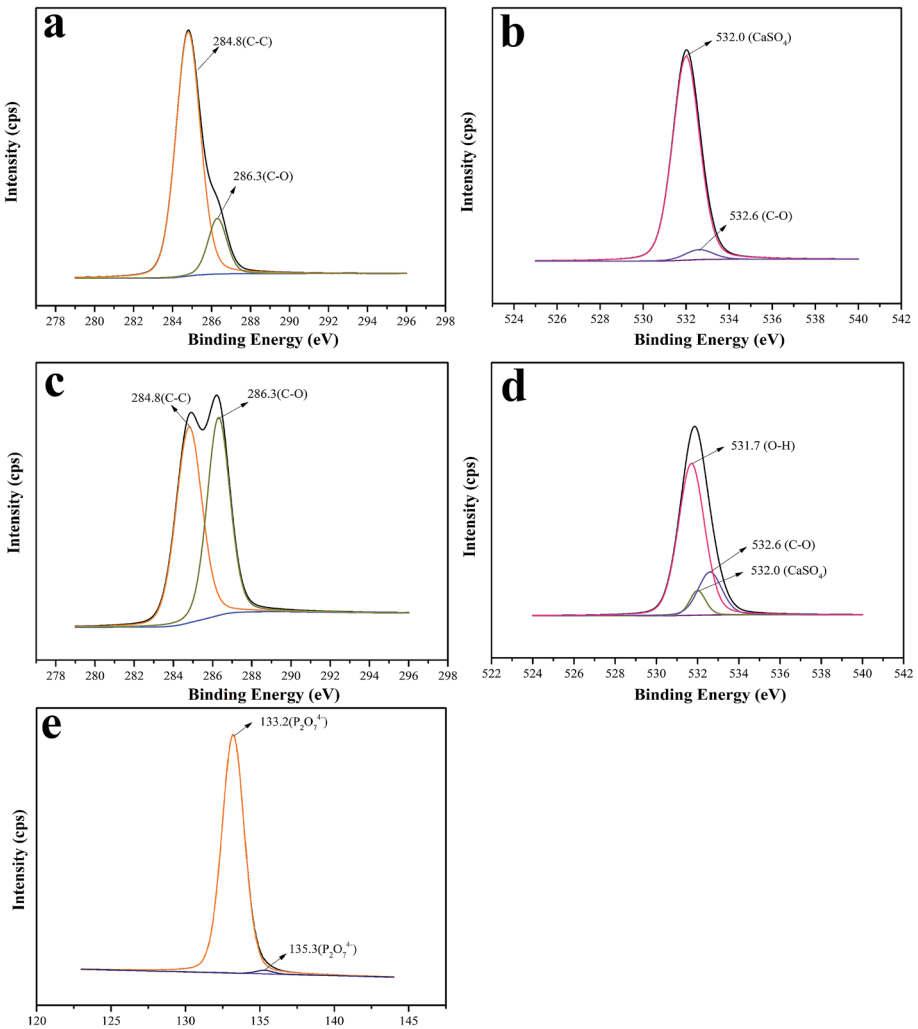

Fig. 7 XPS high-resolution spectra of the C 1s region of (a) CSW and (b) eTi_{4000}-CSW; the O 1s region of (c) CSW and (d) eTi_{4000}-CSW; and the P 2p region of (e) eTi_{4000}-CSW.

It is interesting to note that as the PEG segment length increases, the elongation at break increases, while the Young's modulus and breaking strength increase at first until a maximum is reached in eTi_{4000}-CSW/PVC composite, and decreases thereafter. However, the yield strength is not so sensitive to the PEG segment length, except that eTi_{6000}-CSW/PVC composite shows a slightly lower yield strength. eTi_{4000}-CSW/PVC composite has better performance than other

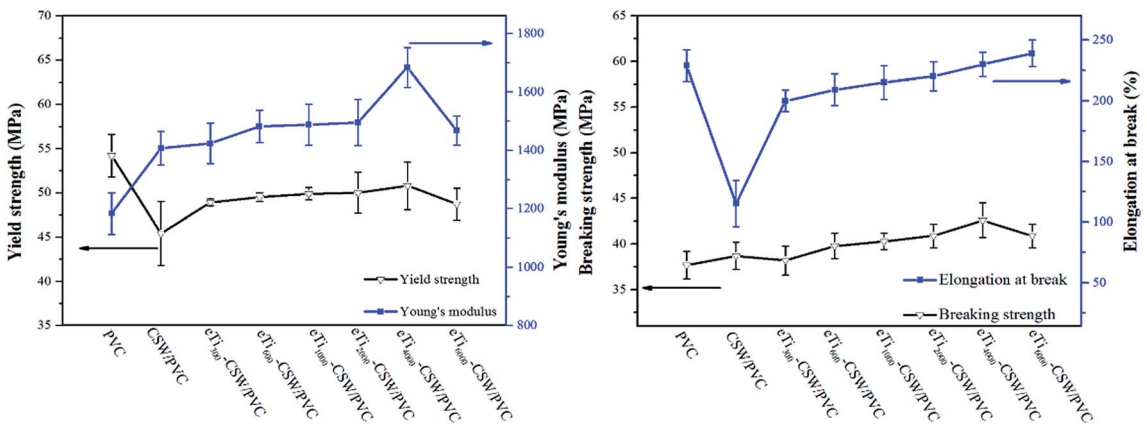

Fig. 8 Mechanical properties of CSW/PVC and mCSW/PVC composites with 10 wt% whisker.

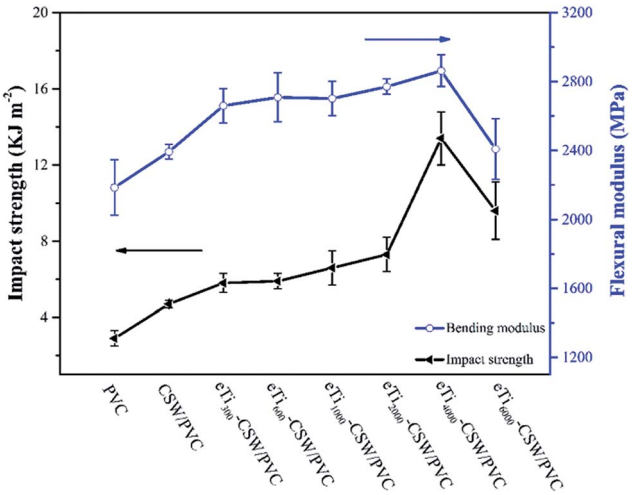

Fig. 9 Impact properties and flexural modulus of CSW/PVC and mCSW/PVC with 10 wt% whisker.

mCSW/PVC composites, and its yield strength, breaking strength, Young's modulus and elongation at break are 50.8 MPa, 42.6 MPa, 1683 MPa and 230%, with an increase of 12.0%, 10.0%, 19.6% and 100% compared with that of the unmodified CSW/PVC composite, respectively. Of the six mCSW/PVC composites prepared in this study, eTi_{4000}-CSW/PVC composite shows the lowest decrease in yield strength compared with pure PVC (50.8 MPa).

It is noted that the increase in interfacial strength is usually accompanied with a decrease in toughness. The presence of a tight bound but stiff interface can lead to high stress concentrations at the interface, thus leading to low impact toughness.[58] However, it should be underlined that both interfacial strength and impact toughness of the composites can be improved simultaneously through an optimum interphase. The impact strength of pure PVC, CSW/PVC and mCSW/PVC composites are shown in Fig. 9. It has been reported that the impact strength increases from 3.0 kJ m^{-2} for pure PVC to 4.7 kJ m^{-2} for CSW/PVC composites.[17,23] Titanate treatment could result in a further increase in the impact strength of mCSW/PVC composites compared with CSW/PVC composite, which is attributed to the improved interfacial compatibility. The impact strength of mCSW/PVC composites increases with increasing PEG segment length, and reaches a maximum of 13.4 kJ m^{-2} in eTi_{4000}-CSW/PVC composite, with an increase of 185% compared to the unmodified CSW/PVC composite. A similar trend is observed in the flexural modulus of mCSW/PVC composites. The maximum flexural modulus is also obtained in eTi_{4000}-CSW/PVC composite (2863 MPa), with an increase of 19.7% compared with that of pure PVC.

The relationship between the mechanical properties and PEG segment lengths can be explained by the difference in the interfacial interaction between titanates with different PEG segments and the matrix, as schematically shown in Fig. 10. Since the titanate content is 3 wt% for all composites, the shorter the PEG segment, the lower the PEG molecular weight, and the more the number of PEG segment bonded on the CSW surface (Fig. 10A). Based on the thermodynamics of mixing, more PEG segments on the mCSW surface can result in a better compatibility between mCSW and the PVC matrix, thus the interfacial affinity will decrease with the increase of PEG segment length in titanates. On the other hand, the entanglement between PEG segment and PVC molecular chain will be intensified with increasing of PEG segment length as long PEG segment can penetrate deeply into the matrix (Fig. 10B), resulting in an increase of the entanglement strength with increasing PEG segment length. The interfacial adhesion strength is determined by the affinity and the entanglement strength of titanates with the matrix. Therefore, their opposite dependence on the PEG segment length leads to the best interfacial interaction and mechanical properties of eTi_{4000}-CSW/PVC composite.

DMA test was performed to demonstrate the effects of titanate coupling agents on the interfacial properties of composites under

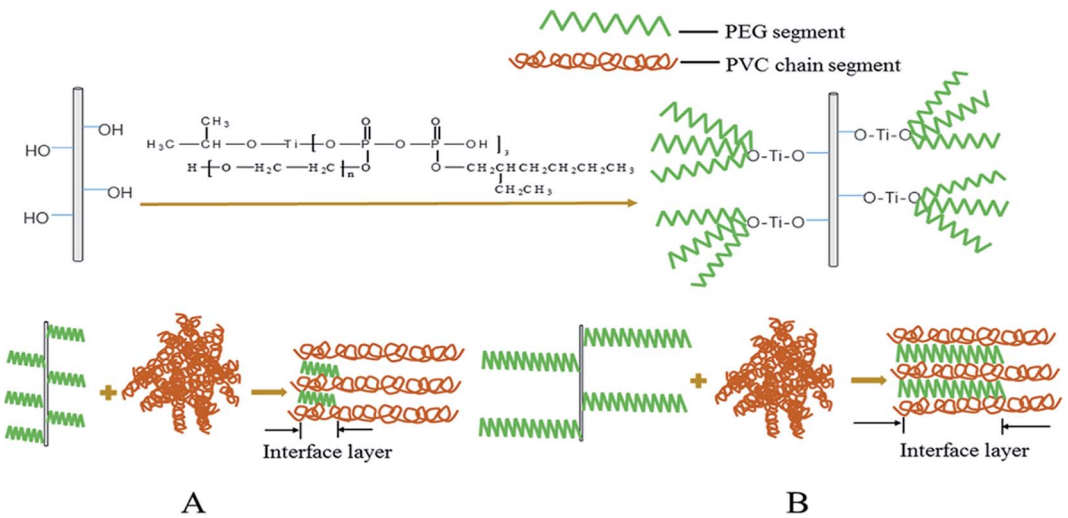

Fig. 10 CSW modified by coupling agent and the interfacial interaction between mCSW and PVC matrix.

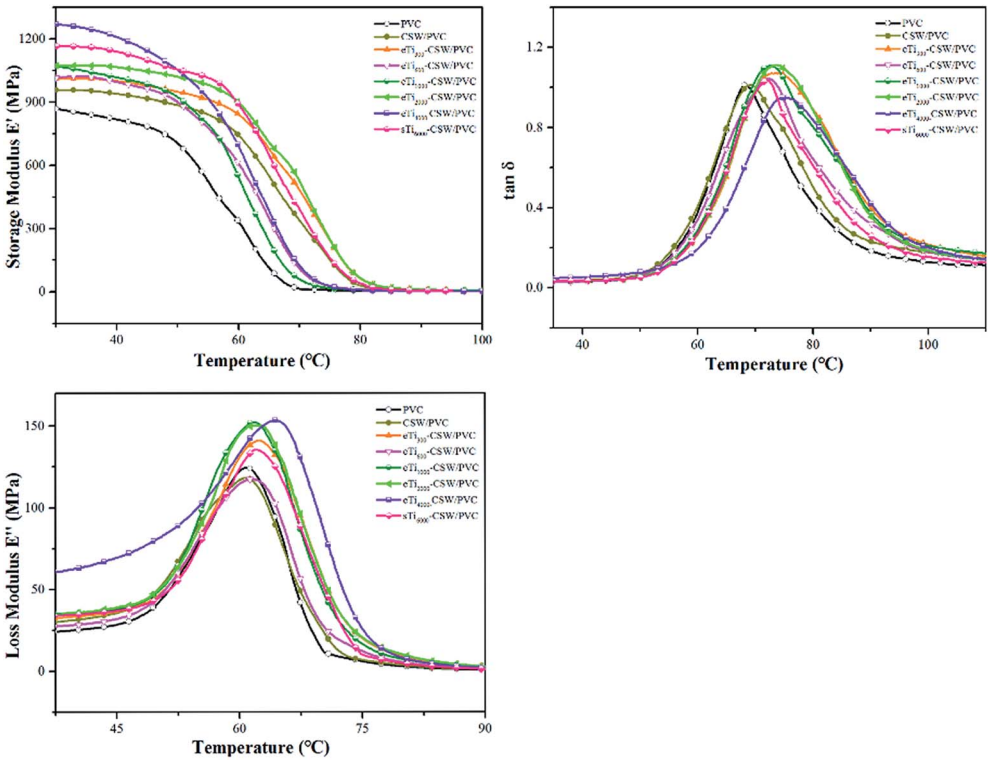

Fig. 11 DMA curves for CSW/PVC and mCSW/PVC composites with 10 wt% whisker.

dynamic loading. The variations of the storage modulus (E'), loss modulus (E'') and tangent δ (tan δ) with temperature for CSW/PVC and mCSW/PVC composites are shown in Fig. 11. It shows that E' increases from 957 MPa for CSW/PVC composite to 1268 MPa for eTi_{4000}-CSW/PVC composite at 30 °C. The tan δ curves show that the T_g of CSW/PVC composite is about 70.0 °C, while that of eTi_{4000}-CSW/PVC composite is about 75.4 °C, with an increase of 5.4 °C. All these results indicate that the interfacial properties can be significantly improved by the modification with the coupling agents synthesized in this study. The dynamic mechanical properties of mCSW/PVC composites are summarized in Tables 3 and 4.

3.4. Morphology

The SEM images of the tensile fracture surfaces of CSW/PVC and mCSW/PVC composites are shown in Fig. 12. For unmodified CSW/PVC composite, the pullout of whiskers from the PVC matrix is observed, and the whiskers are more likely to agglomerate, while for mCSW/PVC composites, the whiskers can adhere tightly to the PVC matrix because of the strong interaction between mCSW and the PVC matrix, which can improve the interfacial properties of the mCSW/PVC composite.[34]

Table 3 Storage modulus of mCSW/PVC composites at 30 °C (MPa)

Coupling agent	eTi_{300}	eTi_{600}	eTi_{1000}	eTi_{2000}	eTi_{4000}	eTi_{6000}
mCSW/PVC	1011	1015	1069	1072	1268	1166

Table 4 Glass transition temperature of mCSW/PVC composites (°C)

Coupling agent	eTi_{300}	eTi_{600}	eTi_{1000}	eTi_{2000}	eTi_{4000}	eTi_{6000}
mCSW/PVC	71.9	72.8	73.0	74.1	75.4	72.1

3.5. Heat resistance

VST reflects the moving ability of chain segments. The more difficult it is for the chain segment to move, the higher the VST will be.[59] Fig. 13 clearly shows that as the chain length increases, the VST of mCSW/PVC composites increases, because these modified whiskers can effectively restrict the mobility of the PVC segments due to their large length-to-diameter ratio[60] and the improved interfacial strength of the composites. However, the VST of eTi_{6000}-CSW/PVC composite decreases slightly due to the longer chains in the coupling agent.

3.6. Thermal stability

The TGA and DTG curves of PVC, CSW/PVC and mCSW/PVC composites are shown in Fig. 14 and 15, respectively. Two weight loss stages are observed for pure PVC, CSW/PVC and mCSW/PVC composites. For pure PVC, the first weight loss stage occurs at about 273 °C, which could be attributed to the dehydrochlorination and the formation of double bonds along the polymer chain.[61] In the temperature range of 292–426 °C, the pure PVC becomes thermally stable again because of the formation of conjugated double bonds after the removal of HCl.[62] A second decomposition stage starts at 426–473 °C, which corresponds to the polyacetylene cracking (the scission of

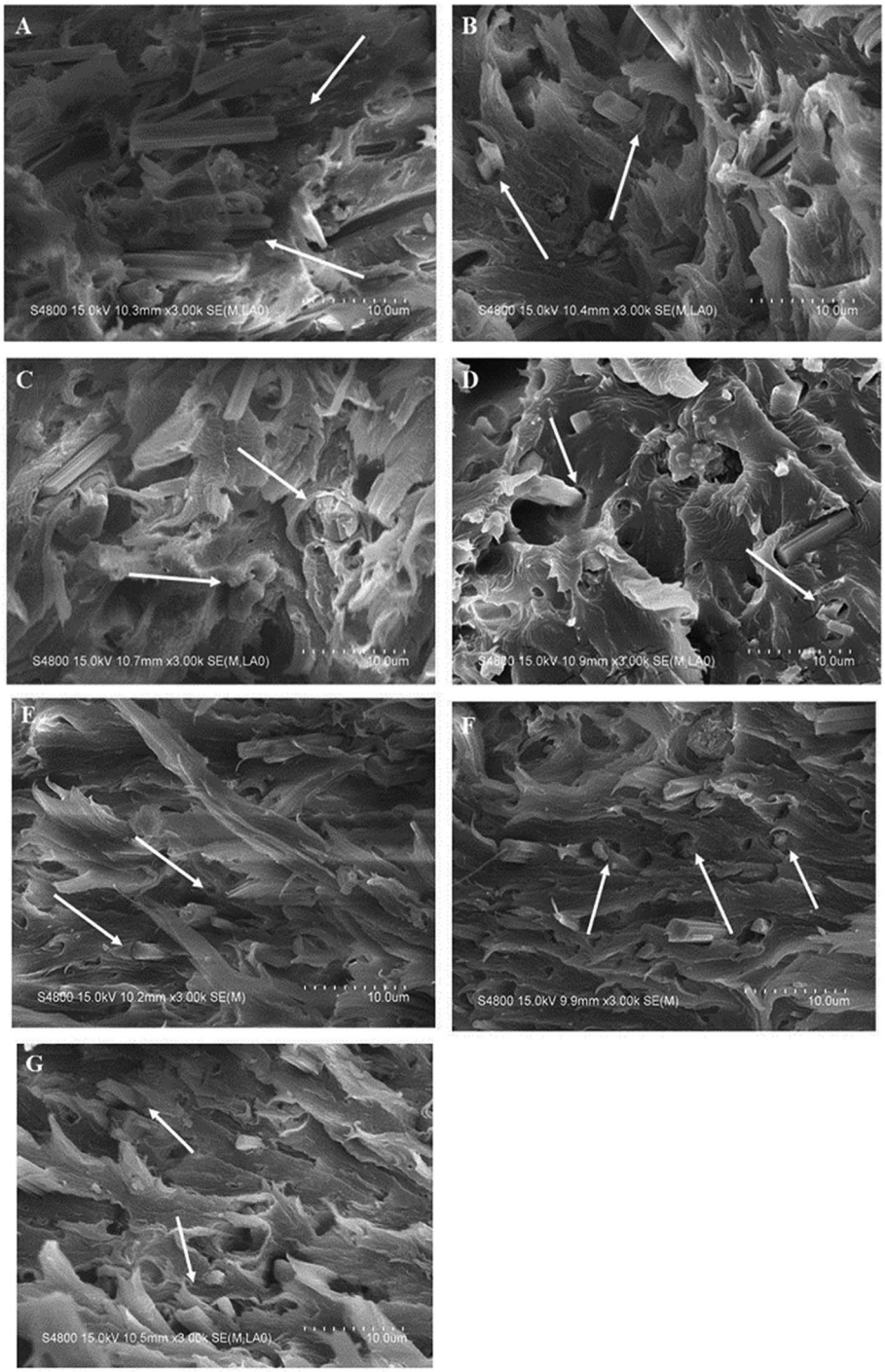

Fig. 12 SEM images of tensile fracture surfaces of (A) CSW/PVC; (B) eTi_{300}-CSW/PVC; (C) eTi_{600}-CSW/PVC; (D) eTi_{1000}-CSW/PVC; (E) eTi_{2000}-CSW/PVC; (F) eTi_{4000}-CSW/PVC; and (G) eTi_{6000}-CSW/PVC composites with 10 wt% whisker.

covalent and multiple bonds). A stable residue (*i.e.*, carbon black) is formed at temperatures higher than 473 °C.[63]

The temperatures of onset decomposition (T_{onset}), rapidest decomposition (T_{rpd}), and 50% weight loss residue (T_{50}) are shown in Table 5. It can be seen that the T_{onset} and T_{rpd} of mCSW/PVC composites are higher than that of CSW/PVC composite and pure PVC, indicating an improved thermal degradation in mCSW/PVC composites. In addition, the T_{onset} and T_{rpd} of mCSW/PVC composites with shorter PEG segments increase more obviously than that with longer PEG segments. The TGA curves also reveal that the T_{50} values of mCSW/PVC composites are higher than that of pure PVC and CSW/PVC composites. This may be because the coupling agents can improve the interface adhesion between CSW and PVC matrix.[63,64]

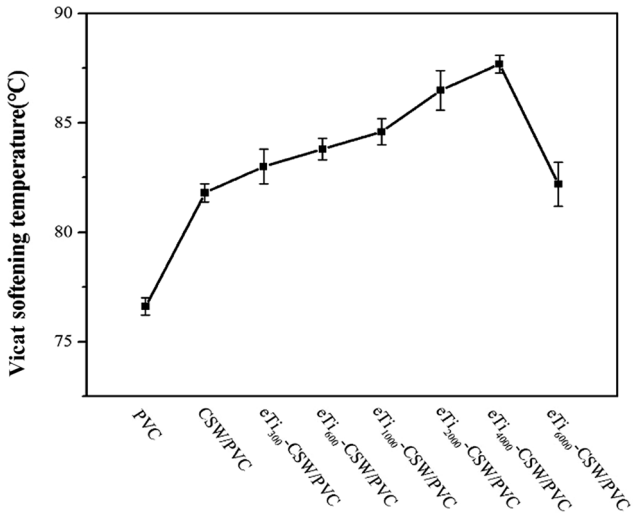

Fig. 13 Vicat softening temperature of CSW/PVC and mCSW/PVC composites with 10 wt% whisker.

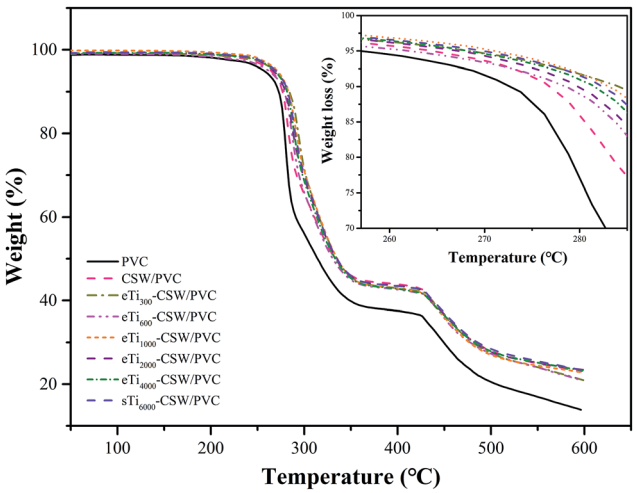

Fig. 14 TGA curves of CSW/PVC and mCSW/PVC composites with 10 wt% whisker.

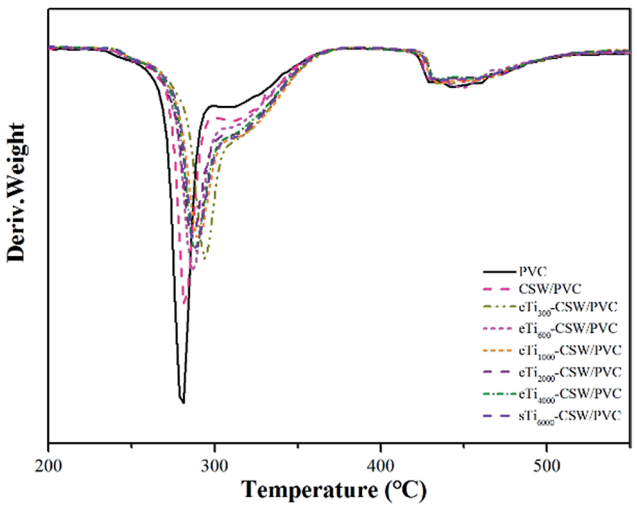

Fig. 15 DTG curves of CSW/PVC and mCSW/PVC composites with 10 wt% whisker.

Table 5 Degradation temperatures of PVC and its composites obtained from the TGA and DTG curves

	Temperature (°C)		
Sample	T_{onset}	T_{rpd}	T_{50}
Pure PVC	273	280	313
CSW/PVC	275	282	331
eTi_{300}-CSW/PVC	280	292	334
eTi_{600}-CSW/PVC	277	287	331
eTi_{1000}-CSW/PVC	277	289	333
eTi_{2000}-CSW/PVC	275	286	333
eTi_{4000}-CSW/PVC	276	286	332
eTi_{6000}-CSW/PVC	275	286	331

4. Conclusion

In this study, new titanate coupling agents with different PEG segment lengths were synthesized to modify CSW in an attempt to improve the interfacial properties of CSW/PVC composites. The results show that these coupling agents could effectively increase the interfacial compatibility and adhesion between CSW and PVC. PEG segment length plays a critical role in the interaction between CSW and the PVC matrix. However, in order for the mCSW/PVC composites to have desirable properties, the flexible chain should be neither too long nor too short. The modification of CSW with these new coupling agents results in a significant improvement in the overall performance of mCSW/PVC composites compared with untreated CSW/PVC composite and pure PVC. Among the six coupling agents, eTi_{4000} performs relatively better. The coupling agents synthesized in this study have the potential to modify various fillers.

Acknowledgements

This research is financially supported by the National Natural Science Foundation of China (U 1507123), the Foundation from Qinghai Science and Technology Department and Thousand Talents Program of Qinghai Province.

References

1 X.-L. Xie, Q.-X. Liu, R. K.-Y. Li, X.-P. Zhou, Q.-X. Zhang, Z.-Z. Yu and Y.-W. Mai, Rheological and mechanical properties of PVC/$CaCO_3$ nanocomposites prepared by *in situ* polymerization, *Polymer*, 2004, **45**, 6665–6673, DOI: 10.1016/j.polymer.2004.07.045.

2 K. Endo, Synthesis and structure of poly(vinyl chloride), *Prog. Polym. Sci.*, 2002, **27**, 2021–2054, DOI: 10.1016/s0079-6700(02)00066-7.

3 C.-H. Chen, C.-C. Teng, S.-F. Su, W.-C. Wu and C.-H. Yang, Effects of microscale calcium carbonate and nanoscale calcium carbonate on the fusion, thermal, and mechanical characterizations of rigid poly(vinyl chloride)/calcium carbonate composites, *J. Polym. Sci., Part B: Polym. Phys.*, 2006, **44**, 451–460, DOI: 10.1002/polb.20721.

4 J. E. Crespo, L. Sanchez, D. Garcia and J. Lopez, Study of the Mechanical and Morphological Properties of Plasticized PVC Composites Containing Rice Husk Fillers, *J. Reinf. Plast. Compos.*, 2007, **27**, 229–243, DOI: 10.1177/0731684407079479.

5 D. Feldman and D. Banu, Contribution to the study of rigid PVC polyblends with different lignins, *J. Appl. Polym. Sci.*, 1997, **66**, 1731–1744, DOI: 10.1002/(sici)1097-4628(19971128)66:9<1731::aid-app11>3.0.co;2-y.

6 D. Wang, L. Shi, Q. Luo, X. Li and J. An, An efficient visible light photocatalyst prepared from TiO_2 and polyvinyl chloride, *J. Mater. Sci.*, 2012, **47**, 2136–2145, DOI: 10.1007/s10853-011-6014-6.

7 N. Wang, Q. She, H. Xu, Y. Yao, L. Zhang, X. Qu and L. Zhang, Preparation and characterization of nano-$CaCO_3$ encapsulated with polyacrylic and its application in PVC toughness, *J. Appl. Polym. Sci.*, 2010, **115**, 1336–1346, DOI: 10.1002/app.30508.

8 Q. Wang, X. Zhang, S. Liu, H. Gui, J. Lai, Y. Liu, J. Gao, F. Huang, Z. Song, B. Tan and J. Qiao, Ultrafine full-vulcanized powdered rubbers/PVC compounds with higher toughness and higher heat resistance, *Polymer*, 2005, **46**, 10614–10617, DOI: 10.1016/j.polymer.2005.08.074.

9 C.-S. Ha, Y. Kim, W.-K. Lee, W.-J. Cho and Y. Kim, Fracture toughness and properties of plasticized PVC and thermoplastic polyurethane blends, *Polymer*, 1998, **39**, 4765–4772, DOI: 10.1016/S0032-3861(97)10326-3.

10 A. M. Hezma, I. S. Elashmawi, A. Rajeh and M. Kamal, Change spectroscopic, thermal and mechanical studies of PU/PVC blends, *Phys. B*, 2016, **495**, 4–10, DOI: 10.1016/j.physb.2016.04.043.

11 Z. Liu, L. Wu, K. Kwok, X. Zhu, Z. Qi, C. Choy and F. Wang, Effects of interfacial adhesion on the rubber toughening of poly(vinyl chloride) Part 2. Low-speed tensile tests, *Polymer*, 2001, **42**, 1719–1724, DOI: 10.1016/s0032-3861(00)00542-5.

12 J. Yu, J. Summers, A. Hiltner and E. Baer, Quasi-brittle to ductile transition in impact-modified PVC, *J. Vinyl Addit. Technol.*, 2004, **10**, 11–16, DOI: 10.1002/vnl.20003.

13 Y. A. El-Shekeil, S. M. Sapuan, M. Jawaid and O. M. Al-Shuja'a, Influence of fiber content on mechanical, morphological and thermal properties of kenaf fibers reinforced poly(vinyl chloride)/thermoplastic polyurethane poly-blend composites, *Mater. Des.*, 2014, **58**, 130–135, DOI: 10.1016/j.matdes.2014.01.047.

14 N. Petchwattana, S. Covavisaruch and D. Pitidhammabhorn, Influences of water absorption on the properties of foamed poly(vinyl chloride)/rice hull composites, *J. Polym. Res.*, 2013, **20**, 1–7, DOI: 10.1007/s10965-013-0172-y.

15 L. Chazeau, J. Cavaillé and P. Terech, Mechanical behaviour above Tg of a plasticised PVC reinforced with cellulose whiskers; a SANS structural study, *Polymer*, 1999, **40**, 5333–5344, DOI: 10.1016/s0032-3861(98)00748-4.

16 S. H. Zhang, W. J. Gan, W. X. Sun, C. J. Ling, X. Wang and Q. F. Li, Study on Structures and Properties of $CaSO_4$ Whiskers/PVC Composites, *Adv. Mater. Res.*, 2011, **335–336**, 234–239, DOI: 10.4028/www.scientific.net/amr.335-336.234.

17 W. Yuan, J. Cui, Y. Cai and S. Xu, A novel surface modification for calcium sulfate whisker used for reinforcement of poly(vinyl chloride), *J. Polym. Res.*, 2015, **22**, 173, DOI: 10.1007/s10965-015-0813-4.

18 Z. Huang, Z. Lin, Z. Cai and K. Mai, Physical and mechanical properties of nano-$CaCO_3$/PP composites modified with acrylic acid, plastics, *Rubber Compos.*, 2013, **33**, 343–352, DOI: 10.1179/174328904X22314.

19 Q. Zhang, H. Yang and Q. Fu, Kinetics-controlled compatibilization of immiscible polypropylene/polystyrene blends using nano-SiO_2 particles, *Polymer*, 2004, **45**, 1913–1922, DOI: 10.1016/j.polymer.2004.01.037.

20 J. Zhang, X. Wang, L. Lu, D. Li and X. Yang, Preparation and performance of high-impact polystyrene (HIPS)/nano-TiO_2 nanocomposites, *J. Appl. Polym. Sci.*, 2003, **87**, 381–385, DOI: 10.1002/app.11302.

21 Y.-x. Zhang, Y.-h. Song and Q. Zheng, Mechanical and thermal properties of nanosized titanium dioxide filled rigid poly(vinyl chloride), *Chin. J. Polym. Sci.*, 2013, **31**, 325–332, DOI: 10.1007/s10118-013-1219-6.

22 X. F. Zeng, W. Y. Wang, G. Q. Wang and J. F. Chen, Influence of the diameter of $CaCO_3$ particles on the mechanical and rheological properties of PVC composites, *J. Mater. Sci.*, 2008, **43**, 3505–3509, DOI: 10.1007/s10853-008-2475-7.

23 W. Yuan, J. Cui and S. Xu, Mechanical Properties and Interfacial Interaction of Modified Calcium Sulfate Whisker/Poly(Vinyl Chloride) Composites, *J. Mater. Sci. Technol.*, 2016, **32**, 1352–1360, DOI: 10.1016/j.jmst.2016.05.016.

24 Y. Wang, Y. Li, A. Yuan, B. Yuan, X. Lei, Q. Ma, J. Han, J. Wang and J. Chen, Preparation of calcium sulfate whiskers by carbide slag through hydrothermal method, *Cryst. Res. Technol.*, 2014, **49**, 800–807, DOI: 10.1002/crat.201400155.

25 X. L. Wang, Y. M. Zhu, Y. X. Han, Z. T. Yuan and W. Z. Yin, Toughening of Polypropylene with Calcium Sulfate Whiskers Treated by Coupling Agents, *Adv. Mater. Res.*, 2009, **58**, 225–229, DOI: 10.4028/www.scientific.net/amr.58.225.

26 H. Kim, Y. Miura and C. W. Macosko, Graphene/Polyurethane Nanocomposites for Improved Gas Barrier and Electrical Conductivity, *Chem. Mater.*, 2010, **22**, 3441–3450, DOI: 10.1021/cm100477v.

27 E. Song, D. Kim, B. J. Kim and J. Lim, Surface modification of $CaCO_3$ nanoparticles by alkylbenzene sulfonic acid surfactant, *Colloids Surf., A*, 2014, **461**, 1–10, DOI: 10.1016/j.colsurfa.2014.07.020.

28 B. Qiao, Y. Liang, T.-J. Wang and Y. Jiang, Surface modification to produce hydrophobic nano-silica particles using sodium dodecyl sulfate as a modifier, *Appl. Surf. Sci.*, 2016, **364**, 103–109, DOI: 10.1016/j.apsusc.2015.12.116.

29 N. G. Shimpi, A. D. Mali and S. Mishra, Property investigation of surface-modified MMT on mechanical and photo-oxidative degradation of viton rubber composites, *Polym. Bull.*, 2016, **73**, 3033–3048, DOI: 10.1007/s00289-016-1639-x.

30 H. Jiang and D. P. Kamdem, Characterization of the surface and the interphase of PVC–copper amine-treated wood composites, *Appl. Surf. Sci.*, 2010, **256**, 4559–4563, DOI: 10.1016/j.apsusc.2010.02.047.

31 C. H. Chen, R. D. Wesson, J. R. Collier and Y. W. Lo, Studies of rigid poly(vinyl chloride) (PVC) compounds. I. Morphological characteristics of poly(vinyl chloride)/chlorinated polyethylene (PVC/CPE) blends, *J. Appl. Polym. Sci.*, 1995, **58**, 1087–1091, DOI: 10.1002/app.1995.070580701.

32 X. Liu, P. Chu and C. Ding, Surface modification of titanium, titanium alloys, and related materials for biomedical applications, *Mater. Sci. Eng., R*, 2004, **47**, 49–121, DOI: 10.1016/j.mser.2004.11.001.

33 A. B. Bourlinos, D. Gournis, D. Petridis, T. Szabó, A. Szeri and I. Dékány, Graphite Oxide, *Langmuir*, 2003, **19**, 6050–6055, DOI: 10.1021/la026525h.

34 W. Yuan, Y. Lu and S. Xu, Synthesis of a New Titanate Coupling Agent for the Modification of Calcium Sulfate Whisker in Poly(Vinyl Chloride) Composite, *Materials*, 2016, **9**, 625, DOI: 10.3390/ma9080625.

35 J. Cui, Y. Cai, W. Yuan, Z. Lv and S. Xu, Preparation of a Crosslinked Chitosan Coated Calcium Sulfate Whisker and Its Reinforcement in Polyvinyl Chloride, *J. Mater. Sci. Technol.*, 2016, **32**, 745–752, DOI: 10.1016/j.jmst.2016.06.006.

36 J.-Y. Cui, Y.-B. Cai, W.-J. Yuan, Z.-F. Lv, C. Zhang and S.-A. Xu, Preparation of PMMA grafted calcium carbonate whiskers and its reinforcement effect in PVC, *Polym. Compos.*, 2015, 1–9, DOI: 10.1002/pc.23873.

37 M. N. Belgacem, P. Bataille and S. Sapieha, Effect of corona modification on the mechanical properties of polypropylene/cellulose composites, *J. Appl. Polym. Sci.*, 1994, **53**, 379–385, DOI: 10.1002/app.1994.070530401.

38 J. Zhu, S. Wei, J. Ryu, M. Budhathoki, G. Liang and Z. Guo, *In situ* stabilized carbon nanofiber (CNF) reinforced epoxy nanocomposites, *J. Mater. Chem.*, 2010, **20**, 4937, DOI: 10.1039/c0jm00063a.

39 S. Sun, C. Li, L. Zhang, H. L. Du and J. S. Burnell-Gray, Effects of surface modification of fumed silica on interfacial structures and mechanical properties of poly(vinyl chloride) composites, *Eur. Polym. J.*, 2006, **42**, 1643–1652, DOI: 10.1016/j.eurpolymj.2006.01.012.

40 S. Yun, Q. Song, D. Zhao, G. Qian, X. Li and W. Li, Study on the inorganic–organic surface modification of potassium titanate whisker, *Appl. Surf. Sci.*, 2012, **258**, 4444–4448, DOI: 10.1016/j.apsusc.2012.01.003.

41 C. Ai Wah, L. Yub Choong and G. Seng Neon, Effects of titanate coupling agent on rheological behaviour, dispersion characteristics and mechanical properties of talc filled polypropylene, *Eur. Polym. J.*, 2000, **36**, 789–801, DOI: 10.1016/s0014-3057(99)00123-8.

42 M. Hajian, G. A. Koohmareh and A. Mostaghasi, Investigation of the Effects of Titanate as Coupling Agent and Some Inorganic Nanoparticles as Fillers on Mechanical Properties and Morphology of Soft PVC, *Int. J. Polym. Sci.*, 2011, **2011**, 1–9, DOI: 10.1155/2011/238619.

43 I. Kemal, A. Whittle, R. Burford, T. Vodenitcharova and M. Hoffman, Toughening of unmodified polyvinylchloride through the addition of nanoparticulate calcium carbonate and titanate coupling agent, *J. Appl. Polym. Sci.*, 2013, **127**, 2339–2353, DOI: 10.1002/app.37774.

44 S. J. Monte and G. Sugerman, The Use of Titanate Coupling Agents for Improved Properties and Aging of Plastic Composites and Coatings, in Polymer Additives, *Polymer Science and Technology Series*, 1984, **26**, 301–341.

45 Z. Feng-e, S. Yan-jiang and Z. Yun-can, Syntheses of polyether-containing titanate and its effect on mechanical properties of polyolefin/$CaCO_3$ blends, *J. Nanjing Univ. Technol.*, 2004, **26**, 61–66.

46 A. K. Mehrjerdi, B. A. Mengistu, D. Åkesson and M. Skrifvars, Effects of a titanate coupling agent on the mechanical and thermo-physical properties of talc-reinforced polyethylene compounds, *J. Appl. Polym. Sci.*, 2014, **131**, 4525–4529, DOI: 10.1002/app.40449.

47 H.-I. Hsiang, C.-C. Chen and J.-Y. Tsai, Dispersion of nonaqueous Co_2Z ferrite powders with titanate coupling agent and poly(vinyl butyral), *Appl. Surf. Sci.*, 2005, **245**, 252–259, DOI: 10.1016/j.apsusc.2004.10.048.

48 W. Liu, Z. Xie and C. Jia, Surface modification of ceramic powders by titanate coupling agent for injection molding using partially water soluble binder system, *J. Eur. Ceram. Soc.*, 2012, **32**, 1001–1006, DOI: 10.1016/j.jeurceramsoc.2011.11.017.

49 B. Singh, A. Verma and M. Gupta, Studies on adsorptive interaction between natural fiber and coupling agents, *J. Appl. Polym. Sci.*, 1998, **70**, 1847–1858, DOI: 10.1002/(sici)1097-4628(19981128)70:9<1847::aid-app24>3.3.co;2-g.

50 D. K. Lavallee, *The chemistry and biochemistry of N-substituted porphyrins*, VCH Publ, Weinheim, 1987.

51 A. J. Margenot, F. J. Calderón, T. M. Bowles, S. J. Parikh and L. E. Jackson, Soil Organic Matter Functional Group Composition in Relation to Organic Carbon, Nitrogen, and Phosphorus Fractions in Organically Managed Tomato Fields, *Soil Sci. Soc. Am. J.*, 2015, **79**, 772, DOI: 10.2136/sssaj2015.02.0070.

52 M. Aioub and M. A. El-Sayed, A Real-Time Surface Enhanced Raman Spectroscopy Study of Plasmonic Photothermal Cell Death Using Targeted Gold Nanoparticles, *J. Am. Chem. Soc.*, 2016, **138**, 1258–1264, DOI: 10.1021/jacs.5b10997.

53 R. K. Brow, Section 1. Structure Review: the structure of simple phosphate glasses, *J. Non-Cryst. Solids*, 2000, **263–264**(1), 1–28, DOI: 10.1016/S0022-3093(99)00620-1.

54 C. D. Wagner, D. A. Zatko and R. H. Raymond, Use of the oxygen KLL Auger lines in identification of surface chemical states by electron spectroscopy for chemical analysis, *Anal. Chem.*, 1980, **52**, 1445–1451, DOI: 10.1021/ac50059a017.

55 C. Paschoal, R. L. Moreira, C. Fantini, M. A. Pimenta, K. P. Surendran and M. T. Sebastian, Raman scattering study of $RETiTaO_6$ dielectric ceramics, *J. Eur. Ceram. Soc.*, 2003, **23**, 2661–2666, DOI: 10.1016/s0955-2219(03)00141-9.

56 J. Taylor, G. M. Lancaster and J. Rabalais, Surface alteration of graphite, graphite monofluoride and Teflon by interaction

with Ar^+ and Xe^+ beams, *Appl. Surf. Sci.*, 1978, **1**, 503–514, DOI: 10.1016/0378-5963(78)90027-2.

57 F. Zhao and Y. Huang, Grafting of polyhedral oligomeric silsesquioxanes on a carbon fiber surface, *J. Mater. Chem.*, 2011, **21**, 3695, DOI: 10.1039/c0jm03128c.

58 S. C. Tjong and Y. Z. Meng, Effect of reactive compatibilizers on the mechanical properties of polycarbonate/poly(acrylonitrile-butadiene-styrene) blends, *Eur. Polym. J.*, 2000, **36**, 123–129, DOI: 10.1016/s0014-3057(99)00044-0.

59 L. Yang, D. Sun, Y. Li, G. Liu and J. Gao, Properties of poly(vinyl chloride) blended with an emulsion copolymer of N-cyclohexylmaleimide and methyl methacrylate, *J. Appl. Polym. Sci.*, 2003, **88**, 201–205, DOI: 10.1002/app.11646.

60 T. Yu, Y. Li and J. Ren, Preparation and properties of short natural fiber reinforced poly(lactic acid) composites, *Trans. Nonferrous Met. Soc. China*, 2009, **19**, s651–s655, DOI: 10.1016/s1003-6326(10)60126-4.

61 H. Djidjelli, T. Sadoun and D. Benachour, Effect of plasticizer nature and content on the PVC stability and dielectric properties, *J. Appl. Polym. Sci.*, 2000, **78**, 685–691, DOI: 10.1002/1097-4628(20001017)78:3<685::aid-app250>3.0.co;2-f.

62 R. Benavides, B. M. Castillo, A. O. Castañeda, G. M. López and G. Arias, Different thermo-oxidative degradation routes in poly(vinyl chloride), *Polym. Degrad. Stab.*, 2001, **73**, 417–423, DOI: 10.1016/s0141-3910(01)00122-7.

63 I. K. Bishay, S. L. Abd-El-Messieh and S. H. Mansour, Electrical, mechanical and thermal properties of polyvinyl chloride composites filled with aluminum powder, *Mater. Des.*, 2011, **32**, 62–68, DOI: 10.1016/j.matdes.2010.06.035.

64 X. Li, B. Lei, Z. Lin, L. Huang, S. Tan and X. Cai, The utilization of bamboo charcoal enhances wood plastic composites with excellent mechanical and thermal properties, *Mater. Des.*, 2014, **53**, 419–424, DOI: 10.1016/j.matdes.2013.07.028.